Relative contributions of severe dopaminergic neuron ablation and dopamine depletion to cognitive impairment

R. Garrett Morgan[a], **Jeffrey T. Gibbs**[a], **Erica J. Melief**[a], **Nadia O. Postupna**[a], **Emily E. Sherfield**[a], **Angela Wilson**[a], **C. Dirk Keene**[a], **Thomas J. Montine**[a], **Richard D. Palmiter**[b,c], and **Martin Darvas**[a]

[a]Department of Pathology, University of Washington School of Medicine, University of Washington, Box 357470, Seattle, WA 98195, USA

[b]Department of Biochemistry, University of Washington School of Medicine, University of Washington, Box 357350, Seattle, WA, 98195, USA

[c]Howard Hughes Medical Institute, University of Washington School of Medicine, University of Washington, Box 357350, Seattle, WA, 98195, USA

Abstract

Parkinson's disease (PD) is characterized by the loss of dopaminergic neurons and produces a movement disorder and cognitive impairment that becomes more extensive with the duration of the disease. To what extent cognitive impairment in advanced PD can be attributed to severe loss of dopamine (DA) signaling is not well understood. Furthermore, it is unclear if the loss of DA neurons contributes to the cognitive impairment caused by the reduction in DA signaling. We generated genetic mouse models with equally severe chronic loss of DA achieved by either extensive ablation of DA neurons or inactivation of DA synthesis from preserved neurons and compared their motor and cognitive performance. Motor behaviors were equally blunted in both models, but we observed that DA neuron ablation caused more severe cognitive deficits than DA depletion. Both models had marked deficits in cue-discrimination learning. Yet, deficits in cue-discrimination learning were more severe in mice with DA neuron ablation and only mice with DA neuron ablation had drastically impaired performance in spatial learning, spatial memory and object memory tests. These results indicate that while a severe reduction in DA signaling results in motor and cognitive impairments, the loss of DA neurons promotes more extensive cognitive deficits and suggest that a loss of additional factors that depend on DA neurons may participate in the progressive cognitive decline found in patients with PD.

Keywords

Dopamine loss; Neurodegeneration; Animal model; Dementia; Parkinson's disease

Introduction

Parkinson's disease (PD) is a chronic progressively debilitating neurodegenerative disease that affects roughly 115 per 100,000 people (Schapira et al., 2014). The hallmark pathological process associated with PD is dysfunction and degeneration of dopamine (DA) neurons in the substantia nigra pars compacta (SNpc) of the midbrain (Samii et al., 2004). The resulting loss of DA projections to the striatum contributes to the characteristic motor symptoms in PD (Fahn, 2003). Additionally, PD is now appreciated to include decline of cognitive abilities, which affects up to 80% of late-stage PD patients, culminating in an estimated 30% prevalence of dementia in PD patients with more than 10 years of disease duration (Aarsland et al., 2009; Maetzler et al., 2009). These cognitive impairments include deficits in visuospatial learning and memory, cognitive flexibility as well as deficits in working memory (Leverenz et al., 2009; Lima et al., 2008; Owen et al., 1993; Williams-Gray et al., 2007).

DA dysfunction in advanced PD may include disruption of DA neurotransmission in viable DA neurons and severe loss of nigro-striatal SNpc DA neurons, and it is unclear how these processes contribute to PD-associated phenotypes (Cheng et al., 2011; Cookson, 2009; Koprich et al., 2010; Lundblad et al., 2012; Nemani et al., 2010). This has important implications for understanding the development of cognitive and motor deficits in late-stage PD, as the actual loss of SNpc DA neurons observed in advanced PD might have effects beyond the mere loss of DA, including inflammatory responses, gliosis and loss of co-transmitter release from DA neurons (Nagatsu and Sawada, 2006; Seutin, 2005; Whitton, 2007). Thus, effective treatment of late-stage, PD-associated deficits may require targeting these processes as well as the loss of DA. Indeed, the addition of drugs that target novel non-DA factors associated with DA neuronal death to standard PD treatment regimens could lead to more effective treatment of symptoms. Additionally, these drugs could help reduce the reliance of pharmaceutic interventions on DA drugs, which have been associated with serious and unwanted side effects like levodopa-induced dyskinesia or DA-receptor agonist mediated complications, including impulse control disorders, nausea, anxiety and insomnia (Antonini et al., 2009; Kalia et al., 2013; Voon et al., 2011). Determining whether DA neuron loss leads to similar or worse PD-associated phenotypes than disrupted DA neurotransmission with comparable levels of DA depletion would greatly improve our understanding of the pathological processes that underlie cognitive and motor deficits in late-stage PD.

To determine the relative contributions of large-scale DA depletion and DA neuron ablation to cognitive and motor impairments, and whether processes involved in DA neuron loss beyond loss of DA lead to PD-associated impairments, we developed two genetic mouse models of severe DA loss. In the first model (DAT:TH-KO), DA synthesis is abolished through genetic inactivation of the tyrosine hydroxylase (*Th*) gene in all DA-transporter (DAT) expressing neurons, which make up the majority of midbrain DA neurons (Darvas et al., 2014b; Henschen et al., 2013). Importantly, in this model DA neurons are still present and otherwise intact. In the second model (DAT-DTR), we genetically targeted expression of the human diphtheria-toxin (DT) receptor to all DAT-expressing neurons, which allows

for controlled and selective cell death of this neuronal population by injection with DT (Postupna et al., 2014). We then compared performance of cognitive and motor behaviors in these two models. Because both models have an equal and severe loss of DA, we have used them as models for DA loss in advanced PD.

Materials and methods

Animals

All animal use procedures were approved by the Institutional Animal Care and Use Committee at the University of Washington. Mice were housed under a 12-h, light–dark cycle in a temperature-controlled room with food and water available ad libitum. Mice with inactivation of the *Th* gene in DAT-expressing neurons (DAT:TH-KO) were generated by crossing mice with two floxed *Th* alleles ($Th^{lox/lox}$) with mice that have one deleted *Th* allele ($Th^{-/+}$) and one allele with Cre recombinase expressed under the control of the Slc6a3 gene encoding DAT ($Slc6a3^{Cre/+}$). DAT:TH-KO mice had the genotype $Th^{-/lox}$-$Slc6a3^{Cre/+}$ and their littermates with the genotype $Th^{lox/+}$-$Slc6a3^{Cre/+}$ were used as wild type (WT) control animals (Darvas et al., 2014b; Henschen et al., 2013). Mice with targeted expression of the human DT-receptor (DAT-DTR) were generated by breeding C57Bl/6 mice with mice that have one allele with DTR expressed under the control of the Slc6a3 gene ($Slc6a3^{DTR/+}$). At the age of 3–5 days, all mice from DAT-DTR breeder cages were injected with DT (50 μg/kg, subcutaneously), which resulted in ablation of DAT-expressing neurons in DAT-DTR mice and had no effect on non-transgenic littermates. DT-injected DAT-DTR mice were used as experimental animals, denoted as DAT-DTR (DT), and DT-injected non-transgenic littermates were used as WT controls. The genetic background for all mice was C57Bl/6J. The number of animals used for each procedure can be found in the figure legends.

Drugs

Diphtheria toxin (List Biological Laboratories, Campbell, CA) was dissolved in saline solution and administered subcutaneously. SKF81297 (Tocris, Minneapolis, MS) and Pramipexole (Sigma-Aldrich, St. Louis, MO) were dissolved in saline solution and administered intraperitoneally (i.p.).

Behavioral procedures

All behavior experiments were performed on 3- to 5-month-old mice of mixed sexes and all mice were group-housed with no mixing of genders. All experiments were performed in a blinded fashion such that the experimenter was unaware of each animal's genotype. Each animal was only used once in any of the water-escape based procedures. Novelty-induced locomotor activity, object memory, open-field exploration and all procedures using SKF 81297 and pramipexole were performed using only experimentally naïve animals. Motor behavior testing was performed in animals that were also later tested using water-escape based procedures. For these animals, the time interval between procedures was at least 7 days.

Novelty locomotion and locomotor effects of DA-receptor agonists were determined using static mouse cages (37.2 cm D × 23.4 cm W × 14 cm H) with 16 photo cells per side (Columbus Instruments, Columbus, OH). Locomotor activity was measured as ambulations (2 consecutive beam interruptions) and summated over a recording period of 90 min. Locomotor activity was recorded on three consecutive days. On each day, animals were first allowed a 30-min habituation period in the behavior testing room to reduce transfer arousal. They were then acclimated to their individual static cages for 90 min to allow them to become accustomed to the novel environment. We used the locomotor activity on the very first day of testing as a measure for novelty induced locomotion. After the 90-min acclimatization period, mice were injected with saline (i.p.) on the first and second day of testing. This procedure served to habituate the animals to the i.p. injection procedure and we used the locomotor activity following saline injection on the second day of testing as an internal reference against which we compared the locomotor effects of the DA-receptor agonists SKF 81297 and pramipexole. On the third day, one group of animals was injected with the D1 DA-receptor agonist SKF 81297 (5 mg/kg i.p.) and another group of animals were injected with the D2/D3 DA-receptor agonist pramipexole (0.5 mg/kg i.p.).

Turn- and cue-discrimination learning were measured in a water-based, U-shaped maze consisting of a stem with two backward bent arms (one white/one black) where an escape platform, not visible from the end of stem, can be placed (Darvas and Palmiter, 2011). Mice were trained for 10 trials per day with a 3–5 min inter-trial interval (ITI) between trials. The left-right orientation of the white and black arms of the maze was alternated every day in a pseudo-random, non-repetitive sequence so that both arms were equally located on either side of the maze for each daily 10-trial block. One cohort of mice was trained for 3 days to learn a turn direction-based water escape strategy (turn-discrimination) and another independent cohort of mice was trained for 4 days to learn a water escape strategy based on the color of the arms (cue-discrimination). For each day, the percentage of correct trials and latencies to reach the platform were recorded and averaged over all 10 trials. When an animal did not enter the correct arm of the maze, we did not remove it from the maze but allowed it to correct its behavior. We employed this measure because we used water escape to motivate learning in our procedure and removing animals from the maze after a wrong decision would have potentially reinforced that decision. In addition, we were interested in the animals' ability to correct wrong decisions, which would be reflected in the overall escape latencies. After completion of this procedure, animals were not used for further behavioral testing.

Spatial learning and memory were measured using a modified version of the Morris water maze procedure (Darvas and Palmiter, 2009; Morris, 1984; Vorhees and Williams, 2006). Mice were trained to locate a platform that was submerged in a circular pool (84 cm diameter) filled with opaque water. Outside the pool spatial cues were provided in the behavior-testing area and no cues were present inside the pool. Over a period of 4 days, animals received 4 training trials (with an ITI of 3–5 min) in which they were released into different locations of the pool. Each trial ended if the animal reached the submerged platform within 90 s. If the animal failed to reach the platform within 90 s, the experimenter gently guided the animal to the platform. In either case, the animal was allowed rest on

top of the platform for 30 s. All trials were recorded with a camera and analyzed using Ethovision video-tracking software (Noldus, Wageningen, The Netherlands). Spatial learning was measured as the latency to reach the submerged platform and was averaged over the 4 trials of each training day. In addition, we used Ethovision software to calculate the average swim speed and path length of animals in the Morris maze. After completion of this procedure, animals were only used for testing of spatial memory (see below).

Spatial memory was measured using animals that were previously trained with our spatial learning procedure: one day after the last training session, mice performed one 90-s probe trial in the Morris maze from which the platform was now removed. Video recordings of the probe trial were analyzed with Ethovision software and spatial memory was scored as the percentage of time spent in the quadrant of the pool where the platform was positioned during training. Spatial memory precision was measured during the probe trial as the average proximity (distance) to the exact location where the platform was positioned during training. After completion of this procedure, animals were not used for further behavioral testing.

Object memory was assessed with the novel-object recognition test (Bevins and Besheer, 2006; Darvas and Palmiter, 2010). Animals were first habituated for 15 min to the circular (45 cm diameter) testing apparatus. One day later, mice were allowed to explore the apparatus with two identical objects placed equidistant from the walls for 3 5-min trials with a 5-min ITI. On the following day, one of the original objects was replaced with a novel object and mice were allowed to explore the apparatus for 15 min. Time spent investigating both the original and novel object during that session was measured and scored as the time when mice made direct contact with an object. Accidental or incidental contacts made by the animals were not counted. Object memory was measured as the preference for the novel object over the original object during exploration of both objects.

Anxiety-related behavior (open field exploration) was determined by analyzing the exploratory behavior of animals during the first 10 minutes of the habituation procedure for the novel-object recognition test, and by testing independent cohorts of experimentally naive mice for 10 minutes in the same experimental apparatus. Video recordings were analyzed with Ethovision software and the time spent in the center area and periphery of the circular testing apparatus was calculated. Anxiety was scored as the time spent in the center area of the apparatus.

Motor coordination. Learning-independent motor coordination was measured using the beam-walk test. Mice traversed a 60 cm cylindrical rod (15 mm in diameter) that was elevated 30 cm above a cushioned table and the number of slips was recorded. The test was performed once. Mice that fell were placed back on the beam at the position where they fell and allowed to continue.

Motor-skill learning. Latency to fall from a rotating rotarod (Rotamex 4/8 system, Columbus Instruments) was recorded over 3 consecutive days with 4 trials per day and an ITI of 10 min. For each trial, mice were placed on the rotating rod, which began at 4 rpm and accelerated to 40 rpm over the course of 5 min.

Quantification of DAT and DA

Brains were collected 10–15 days after the last behavior test was finished. For quantification of DAT content in the midbrain, we dissected the SNpc, ventral tegmental area (VTA), and for quantification of DAT content in the striatum, we collected tissue punches from the dorsal and ventral regions of the striatum, as well as whole cerebellum samples to use as a negative control. Tissue was immediately frozen in liquid nitrogen and stored at −80 °C. Protein extractions from dissected tissue and quantification of DAT by ELISA were performed as previously described (Darvas et al., 2014a). In short, Samples were homogenized in RIPA buffer (Sigma-Aldrich) containing Complete Mini protease inhibitors (Roche Applied Science), centrifuged at $1,000 \times g$ for 10 min and the supernatants were collected for further analysis. After determining the protein concentration in the supernatant, using a bicinchoninic assay (Thermo Scientific), DA-transporter expression was quantified by ELISA. Wells of a 96-well plate were coated with monoclonal rat anti DA-transporter antibody (1:500, Abcam), washed, blocked with 5% bovine serum albumin, washed and then incubated with 20 μg total protein. Then wells were washed, incubated with polyclonal rabbit anti DA-transporter antibody (1:20,000, Abcam), washed and incubated with a horse-radish peroxidase-conjugated, donkey anti-rabbit antibody (1:500, Jackson ImmunoResearch). After another wash samples were incubated with TMB solution (R & D Systems). The resulting color reaction was stopped by addition of 2N sulfuric acid and then absorption at 450 nm was measured. DA content was measured in tissue punches (1 mm diameter, 2 mm thick) that were obtained from the prefrontal cortex, amygdala, hippocampus and striatum. Tissue punches were immediately frozen in liquid nitrogen and stored at −80 °C. HPLC coupled with electrochemical detection was used to measure DA content in tissue punches from all brain regions. We also measured 3,4-dihydroxyphenylacetic acid (DOPAC) and norepinephrine levels in striatal tissue punches.

Statistical analyses

All tests that involve multiple trials/groups were analyzed by appropriate analysis of variance (ANOVA, one-way or 2-way) or 2-way repeated measures (RM) ANOVA. Significant effects were further analyzed with Tukey's post-hoc test. All statistical testing was performed with GraphPad Prism software (GraphPad, La Jolla, CA). Any group differences with an alpha of 0.05 or less were considered significant.

Results

Because we did not observe any differences between WT mice that received DT injections and non-injected WT mice, we grouped them together for the presentation of our data.

Expression of DAT in the midbrain and striatum

We generated two different models of severe DA loss. Loss of DA through inactivation of the *Th* gene in DAT-expressing neurons (DAT:TH-KO) and loss of DA through DT-mediated ablation of DAT expressing neurons (DAT-DTR). To validate the difference between our models, we compared expression of DAT, which is a marker for most DA neurons in the midbrain.

ANOVA of DAT expression in the midbrain revealed significant effects of group in the SNpc ($F_{3,23}$ = 32.75, p < 0.01; Fig. 1A) and the VTA ($F_{3,21}$ = 15.39, p < 0.01; Fig. 1B). Whereas DAT:TH-KO mice had DAT expression in both SNpc and VTA that was indistinguishable from WT controls (Fig. 1A–B), DAT-DTR (DT) mice had significantly reduced levels of DAT expression in the SNpc and VTA when compared with WT and DAT:TH-KO mice (Fig. 1A–B). DAT is not expressed highly in the cerebellum (reduced expression when compared to SNpc and VTA, each p < 0.01) and we therefore used WT cerebellum as a "negative control". Importantly, DAT expression in SNpc and VTA of DAT-DTR (DT) mice was not different from DAT expression in the cerebellum of WT mice (Fig. 1A–B), and DAT expression in either SNpc or VTA of DAT:TH-KO and WT mice was significantly higher than that in the cerebellum (p < 0.01; Fig. 1A–B). Interestingly, in DAT-DTR (DT) mice, DAT expression in the VTA was slightly elevated (p < 0.05) when compared with the SNpc. Yet, expression in SNpc and VTA of DAT-DTR (DT) mice was still undistinguishable from our cerebellar negative control. We found no significant differences of DAT expression between SNpc and VTA in any of the other groups.

The striatum receives major innervation from midbrain DA neurons and contains a high number of DAT-expressing fibers. ANOVA of DAT expression in the striatum revealed significant effects of group in the dorsal striatum ($F_{3,20}$ = 26.41, p < 0.01; Fig. 1C) and the ventral striatum ($F_{3,20}$ = 17.16, p < 0.01; Fig. 1D). DAT-DTR (DT) mice had DAT-expression in both the dorsal and ventral striatum that was significantly less than in all other groups (each p < 0.05) and that was undistinguishable from DAT expression in the negative control (cerebellum). DAT:TH-KO mice had DAT expression in both dorsal and ventral striatum that was reduced when compared to WT controls (each p < 0.05), but significantly higher than in samples from DAT-DTR (DT) mice or the cerebellum (each p < 0.05). We found no significant differences between DAT expression in the dorsal and ventral striatum of any group.

Taken together, we conclude that DAT-containing neurons in the midbrain and DATcontaining neuronal fibers in the striatum were drastically reduced in DAT-DTR (DT) mice. In contrast, DAT-containing midbrain neurons were intact in DAT:TH-KO and DAT-containing striatal neuronal fibers were reduced to ~ 67% of WT.

DA content

To confirm that, despite their difference in DAT-expression, our two models have a similar loss of DA synthesis we compared tissue content of DA in the major innervation fields of midbrain DA neurons: prefrontal cortex, hippocampus, amygdala and striatum.

There were no significant differences in DA content in the prefrontal cortex ($F_{2,33}$ = 0.18; Fig. 2A) or hippocampus ($F_{2,13}$ = 0.11; Fig. 2B) for all groups of mice. In the amygdala, ANOVA showed a statistically significant effect of group for DA content ($F_{2,39}$ = 7.54, p < 0.01; Fig. 2C). DAT:TH-KO mice had lower DA content in the amygdala than WT mice (Fig. 2C), and DAT-DTR (DT) mice had significantly reduced amygdala DA content (~74%) compared with WT mice (p < 0.01; Fig. 2C). There were no significant differences in DA content in the amygdala between DAT:TH-KO and DAT-DTR (DT) mice (Fig. 2C). In the striatum, we found significant effects of group for DA levels ($F_{2,46}$ = 182.0, p < 0.01;

Fig. 2D). Both DAT:TH-KO and DAT-DTR (DT) mice exhibited approximately 90% reductions in DA content in the striatum compared with WT mice (both $p < 0.01$; Fig. 2D). There were no differences in striatal DA content between DAT:TH-KO and DAT-DTR (DT) mice (Fig. 2D). In addition, we found significant effects of group for the DOPAC/DA ratio in the striatum ($F_{2,40} = 27.15$, $p < 0.01$; Fig. 2E). Both DAT:TH-KO and DAT-DTR (DT) mice exhibited approximately 3–4 fold increased DOPAC/DA ratios in the striatum compared with WT mice (both $p < 0.01$; Fig. 2E). There were no differences in the striatal DOPAC/DA ratio between DAT:TH-KO and DAT-DTR (DT) mice (Fig. 2D). There were no significant differences in norepinephrine content in the striatum from all groups of mice ($F_{3,34} = 0.15$; Fig. 2F).

Taken together, both models had equally severe striatal loss of DA similar to that seen in advanced PD(Fearnley and Lees, 1991). Since the pattern and extent of DA loss in DAT:TH-KO were similar to DAT-DTR mice differences between our models accrue from factors other than mere loss of DA synthesis.

Response to DA receptor agonists

To examine whether loss of DA or loss of DA neurons differ in their ability to respond to DA-receptor agonists, we examined the locomotor response of both models to D1 (SKF 81297) and D2/D3 (pramipexole) DA receptor agonists (Kim et al., 2000).

Two-way ANOVA of locomotor activity of saline- and SKF 81297-treated mice (Fig. 3A) revealed significant effects of treatment ($F_{1,63} = 117.5$, $p < 0.01$), group ($F_{2,63} = 10.02$, $p < 0.01$) and treatment×group interaction ($F_{2,63} = 10.07$, $p < 0.01$). Injection of SKF 81297 significantly increased locomotor activity in all groups of mice as compared with saline treatment (all $p < 0.01$; Fig. 3A). Although all groups of animals had no statistically significant differences in their response to saline treatment (Fig. 3A), DAT:TH-KO and DAT-DTR(DT) mice exhibited at least 67% more ambulations in response to SKF 81297 treatment than treated WT control mice (all $p < 0.01$; Fig. 3A). There were no differences in activity between DAT:TH-KO and DAT-DTR (DT) mice following SKF 81297 treatment (Fig. 3A).

Two-way ANOVA of locomotor activity by saline and pramipexole treated mice (Fig. 3B) revealed significant effects of treatment ($F_{1,64} = 35.98$, $p < 0.01$), group ($F_{2,64} = 24.41$, $p < 0.01$) and treatment × group interaction ($F_{2,64} = 22.99$, $p < 0.01$). However, whereas pramipexole-treated WT mice had ~90% reduced locomotor activity compared with saline ($p < 0.05$; Fig. 3B), DAT:TH-KO and DAT-DTR (DT) mice increased their locomotor activity ~198% following pramipexole treatment as compared with saline (each $p < 0.05$; Fig. 3B). There were no significant differences in the pramipexole-induced increase of activity between DAT:TH-KO and DAT-DTR (DT) mice (Fig. 3B).

We conclude that both these models displayed equivalent locomotor hypersensitivity to DA-receptor agonists.

Turn- and cue-discrimination learning

To ascertain differences between both models in egocentric and cue-dependent associative learning, we tested them in two water-escape based learning paradigms: 3 days of turn-based and 4 days of cue-based discrimination training in a U-maze.

Two-way RM ANOVA of correct trials during training of the turn-based, water-escape strategy (Fig. 4A) showed significant main effects of time ($F_{2,142} = 139.6$, $p < 0.01$) and group ($F_{2,71} = 8.26$, $p < 0.01$), but not of time × group interaction ($F_{4,142} = 1.91$). Post-hoc comparisons confirmed that DAT:TH-KO and DAT-DTR (DT) mice had ~15% fewer correct trials than WT on the first training day (each $p < 0.05$), and DAT:TH-KO mice had ~15% fewer correct trials than WT mice ($p < 0.01$) on the second training day. 2-way RM ANOVA of escape latencies during training of the turn-based water-escape strategy (Fig. 4B) revealed significant main effects of time ($F_{2,142} = 43.50$, $p < 0.01$), group ($F_{2,71} = 5.85$, $p < 0.01$) and of time × group interaction ($F_{4,142} = 4.74$, $p < 0.01$). Post-hoc comparisons confirmed that DAT-DTR (DT) mice had escape latencies that were ~45 s longer than WT mice on the first training day ($p < 0.01$) and escape latencies that were ~23 s longer than WT mice on the second training day ($p < 0.01$). All other escape latencies on days 1–3 did not differ significantly.

Two-way RM ANOVA of correct trials during training of the cue-based, water-escape strategy (Fig. 4C) showed significant main effects of time ($F_{3,87} = 13.82$, $p < 0.01$), group ($F_{2,29} = 26.71$, $p < 0.01$) and of time×group interaction ($F_{6,87} = 4.99$, $p < 0.01$). Post-hoc comparisons confirmed that on training day 1 only DAT-DTR (DT) mice had ~20% fewer correct trials than WT mice ($p < 0.01$) and that on training days 2–4 both DAT:TH-KO and DAT-DTR (DT) mice had ~30–40% less correct trials than WT mice (all $p < 0.01$). There was no significant difference in correct trials between DAT:TH-KO and DAT-DTR (DT) mice. Two-way RM ANOVA of escape latencies during training of the cue-based water-escape strategy (Fig. 4D) revealed significant main effects of time ($F_{3,87} = 8.82$, $p < 0.01$), group ($F_{2,29} = 20.45$, $p < 0.01$) and of time × group interaction ($F_{6,87} = 3.02$, $p < 0.05$). Post-hoc comparisons confirmed that DAT-DTR (DT) mice had escape latencies that were significantly longer (~140–230 s) than those of WT mice on all training days (all $p < 0.01$). Escape latencies by DAT-DTR (DT) mice were also significantly longer than latencies by DAT:TH-KO mice (92–159 s) on all training days ($p < 0.05$). Although escape latencies by DAT:TH-KO mice were elevated (27–42 s) when compared with WT mice, these differences did not reach statistical significance on any training day. Interestingly, while WT mice decreased their escape latencies during training ($p < 0.01$), DAT:TH-KO and DAT-DTR mice had non-changing escape latencies on all training days.

Taken together, these results suggest a mild defect in turn-based, water-escape behavior by DAT:TH-KO and DAT-DTR (DT) mice, and a severe learning deficit for cue-based water escape in DAT:TH-KO and DAT-DTR (DT) mice. Furthermore, DAT-DTR (DT) mice had a severe performance deficit during training of the cue-based water-escape task.

Spatial learning

To uncover potential differences between the models in spatial learning, we employed a 4-day training procedure using the Morris water maze. We also used this procedure to investigate water-related motor abilities of both models.

Two-way RM ANOVA of latencies to reach the submerged platform during training in the Morris water maze (Fig. 4E) revealed significant main effects of time ($F_{3,93} = 47.13$, $p < 0.01$), group ($F_{2,31} = 19.19$, $p < 0.01$) and of time × group interaction ($F_{6,93} = 6.73$, $p < 0.01$). Post-hoc comparisons confirmed that DAT-DTR (DT) mice had escape latencies that were significantly longer (~30–62 s) than those of WT and DAT:TH-KO mice on training days 2–4 (all $p < 0.01$). More important, whereas WT and DAT:TH-KO mice decreased their latencies during training ($p < 0.05$), DAT-DTR mice had the same average latency (~80 s) on every training day.

To better understand the nature of deficits observed in turn- and cue-based water escape learning and in spatial learning, we also analyzed swim speed in the Morris water maze (Fig. 4F). Two-way RM ANOVA of average swim speed in the Morris maze showed significant effects of group ($F_{2,27} = 3.54$, $p < 0.05$) and of time × group interaction ($F_{6,81} = 3.76$, $p < 0.01$), but not of time ($F_{3,81} = 0.64$). Post-hoc comparisons revealed that DAT-DTR (DT) mice had significantly reduced swim speeds (~47%) on training days 2–3 compared with WT and DAT:TH-KO mice (each $p < 0.05$). Although the swim speed by DAT-DTR (DT) mice was still reduced on day 4, this difference was only statistically significant when compared to DAT:TH-KO mice ($p < 0.05$).

We conclude that spatial learning performance was intact in DAT:TH-KO mice and completely blunted in DAT-DTR (DT) mice. Although swimming ability was decreased in DAT-DTR (DT) mice, the magnitude of that decrease was not fully sufficient to completely explain performance deficits observed in spatial learning and in the previous test for cue-based water escape.

Spatial memory, object memory and anxiety

Spatial memory was assessed in all animals that previously underwent the spatial learning procedure in the Morris water maze by subjecting them to a probe trial without platform 24 h after their last training trial. Object memory was tested using the novel-object recognition test with an independent cohort of mice.

Two-way ANOVA of the time spent in each of the quadrants of the Morris water maze during the probe trial (Fig. 5A) showed significant effects of quadrant location ($F_{3,128} = 8.39$, $p < 0.01$) and of quadrant location × group interaction ($F_{6,128} = 8.13$, $p < 0.01$). Further post-hoc analysis of quadrant preferences confirmed that WT mice preferred the quadrant in which the escape platform was located during training trials (Q4) over all three other quadrants (all $p < 0.01$). DAT:TH-KO mice preferred quadrant Q4 over two of the other quadrants ($p < 0.05$) and DAT-DTR (DT) mice had no preference for quadrant Q4. Analysis of the average proximity to the exact platform location (Fig. 5B) by ANOVA showed a significant group effect ($F_{2,31} = 17.03$, $p < 0.01$). Further post-hoc analysis confirmed that the average proximity to the exact platform location was increased by ~9 cm in DAT:TH-

KO mice ($p < 0.05$) and increased by ~15 cm in DAT-DTR (DT) mice ($p < 0.01$) when compared to WT mice. The difference between DAT:THKO and DAT-DTR (DT) mice was not significant.

In the novel-object recognition test (Fig. 5C), only WT and DAT:TH-KO mice spent significantly more time exploring the novel object during the preference choice test, as confirmed with a *t* test for differences of mean preference from 50% (each $p < 0.05$). ANOVA of the percentage of exploration time spent investigating the novel object in the preference choice test revealed a significant group effect ($F_{2,31} = 6.99$, $p < 0.01$). Post-hoc analysis confirmed that DAT-DTR (DT) mice had a significant reduction of their mean preference when compared to WT ($p < 0.05$) and to DAT:TH-KO mice ($p < 0.05$). ANOVA of the total time spent exploring both objects in the preference choice test (Fig. 5D) revealed a significant group effect ($F_{2,31} = 8.97$, $p < 0.01$). Post-hoc analysis confirmed that both DAT:TH-KO and DAT-DTR (DT) mice spent less time ($p < 0.01$) exploring both objects when compared to WT mice.

To determine if the observed exploration deficits by DAT-DTR mice in the Morris water maze or by DAT:TH-KO mice in the object-recognition test were influenced by altered exploration of novel environments in general, we measured novelty-induced general locomotor activity (Fig. 5E). ANOVA of ambulation during novelty-induced locomotor activity failed to show a significant effect of group ($F_{3,52} = 0.37$).

To rule out potential confounds of our cognitive data that are related to anxiety, we also analyzed open-field exploration during the initial habituation phase of our novel objectrecognition procedure. Two-way ANOVA of the time spent in either the center or periphery of the circular arena used for the novel-object recognition procedure (Fig. 5F) showed significant effects of zone (center vs. periphery, $F_{1,94} = 731.7$, $p < 0.01$), of zone × group interaction ($F_{2,94} = 15.88$, $p < 0.01$), but not of group alone ($F_{2,94} = 0.01$). Although all groups spent significantly more time in the periphery than in the center (all $p < 0.01$), DAT:TH-KO mice spent slightly less time (~77 s) in the periphery zone than WT mice.

We conclude that while DAT:TH-KO mice had roughly intact spatial memory for the overall area where the platform was located, their precision memory for the exact location was deficient. Unsurprisingly, due to their failure to learn the location of the platform during training, DAT-DTR (DT) mice exhibited a severe spatial memory impairment. While DAT:TH-KO mice had ~50% reduction of overall object exploration when compared to WT mice, they still showed a preference for the novel object. In contrast, DAT-DTR mice explored both objects, but showed no preference. We observed no lack of novelty-induced general activity or an obvious anxiety phenotype that might account for the performance deficits in spatial and object memory.

Motor performance

We tested two different motor behaviors: learning-independent motor coordination (beam walk procedure) and motor learning (rotating rotarod).

ANOVA of the number of slips during the beam-walk test (Fig. 6A) revealed a significant effect of group ($F_{2,42} = 17.85$, $p < 0.01$), and post-hoc comparisons confirmed that DAT:TH-KO mice had significantly more slips (~9) than WT mice and that DAT-DTR (DT) mice had more (~5) slips than WT mice (each $p < 0.01$). There were no differences in the number of slips from the beam between DAT:TH-KO and DAT-DTR (DT) mice.

Two-way RM ANOVA of latencies to fall from the rotating rotarod (Fig. 6B) showed significant main effects of time ($F_{11,715} = 7.06$, $p < 0.01$), group ($F_{2,65} = 94.82$, $p < 0.01$) and of time × group interaction ($F_{22,715} = 6.23$, $p < 0.01$). Post-hoc comparisons confirmed that DAT-DTR (DT) and DAT:TH-KO mice had significantly reduced fall latencies compared with WT mice on training trials 2–11 (all $p < 0.01$). There were no differences in the latency to fall between DAT:TH-KO and DAT-DTR (DT) mice.

Taken together, although DAT:TH-KO and DAT-DTR (DT) mice had normal locomotor responses to novelty, both learning-independent and learning-dependent motor behaviors were severely impaired in both models.

Gender differences

We did not observe any gender differences in any of our tests.

Discussion

In this study we investigated the contributions of DA neuron ablation and severe DA depletion on cognitive and motor impairments and determined whether processes involved in DA neuron loss beyond loss of DA synthesis lead to more severe behavioral deficits. In our previously published work, we investigated mouse models with mild (up to 30% loss of DA) and moderate (30–70% loss of DA) reduction of striatal DA levels, a reduction similar to that observed in early to mid-stage PD (Darvas et al., 2014a; Fearnley and Lees, 1991; Scherman et al., 1989). In the current study, we wanted to investigate whether a more severe DA loss, similar to that observed on advanced PD (Fearnley and Lees, 1991; Scherman et al., 1989), further exacerbates cognitive deficits related to DA loss. We used a previously developed genetic mouse model (DAT:TH-KO) in which *Th* gene inactivation in DAT-expressing neurons causes permanent and severe loss of striatal DA while leaving DA neurons intact (Henschen et al., 2013). We compared this model with another mouse model developed in our lab (DAT-DTR mice) in which administration of DT causes irreversible lesion of DAT-expressing neurons that results in severe loss of striatal DA and striatal DA fibers (Postupna et al., 2014). Both approaches target the same population of DA neurons and produced an equally severe loss of striatal DA that is similar to the loss of DA observed in advanced PD (Fearnley and Lees, 1991; Scherman et al., 1989). Because cognitive performance declines more as PD progresses, even resulting in PD with dementia (PDD) in some cases, we examined our models using procedures that test cognitive behaviors that are similar to those affected in PD and PDD together with tests for motor ability (Leverenz et al., 2009; Maetzler et al., 2009). Interestingly, while intact midbrain DAT expression in DAT:TH-KO mice suggests that DA neurons are intact, striatal levels of DAT expression in DAT:TH-KO mice was reduced, reflecting potential adaptive changes in the striatum to the severe loss of DA synthesis.

Importantly, we did not observe any decrease in DA levels in the prefrontal cortex and hippocampus in either of our models. This finding is in agreement with reports providing evidence that DAT expression is very low or absent in the prefrontal cortex or hippocampus (Borgkvist et al., 2012; Lammel et al., 2008). Furthermore, consistent with reports of low DAT-expression in the amygdala (Lammel et al., 2008), we found a ~50% reduction of DA in the amygdala of DAT-DTR (DT) mice. Therefore, we suggest that although DA signaling in non-striatal areas contributes to cognitive behaviors similar to those examined in this study, any deficits observed in our models most likely accrue from loss of striatal DA and/or loss of DA neurons that project to the striatum (Brozoski et al., 1979; D'Esposito, 2007; Ragozzino, 2002; Retailleau et al., 2013).

Both of the models displayed similarly increased locomotor activity after administration of D1 and D2/D3 DA-receptor agonists, presumably mediated by hypersensitive striatal DA-receptors (Bamford et al., 2004; Kim et al., 2000). This result suggests that adaptations related to DA-receptor-mediated signaling in pre- and post-synaptic striatal neurons are equivalent in the two models of severe DA loss.

Despite these similarities between the models, analysis of cognitive behaviors revealed significant differences between severe DA neuron ablation and DA depletion. Although severe loss of DA neurons and severe loss of DA both resulted in minor deficits in egocentric learning and in markedly impaired cue-dependent associative learning, DAT-DTR (DT) mice performed significantly worse in the cue-dependent associative learning task than DAT:TH-KO mice. While DAT:TH-KO mice were able to correct erroneous water-escape choices, DAT-DTR (DT) mice were far less able to correct their choices, reflected by their immense delays to disengage from wrong decisions and to initiate a new choice. We further confirmed a difference between the models in spatial learning, where DAT-DTR (DT) mice also failed to learn the behavioral task, again with a performance deficit that can only partially be ascribed to impaired motor ability. Most important, DAT:TH-KO and DAT-DTR (DT) explored the water U-maze, were able to learn the turn-based escape strategy and executed the turn-based water escape within 20–60s. We therefore believe that poor performance in the cue-based escape strategy task and in the Morris water maze is only partly due to poor motor ability but rather resembles cognitive impairment corresponding to bradyphrenia and cognitive rigidity, both of which are also part of the PD-related concept of subcortical dementia (Kehagia et al., 2010).

As expected, probably due their spatial-learning deficit, DAT-DTR (DT) mice had severe spatial memory impairment. However, although we have previously shown that complete lack of DA in all brain regions causes blunted spatial learning and memory (Darvas and Palmiter, 2010), mice with severe loss of striatal DA and intact DA neurons (DAT:TH-KO) performed remarkably well in the same spatial learning and memory task. This difference could either reflect the spatial extent of DA loss (striatum vs. all DA-receiving brain regions), or result from the small amount of residual striatal DA in DAT:TH-KO mice. Interestingly, we confirmed a deficit in object-recognition memory only in DAT-DTR mice, which was not due to a lack of object exploration or of novelty-induced motor activity but rather implicates a role for midbrain DA neurons in mediating object-memory.

Interestingly, motor behaviors were equally affected in both models, as evidenced by severely impaired performance of learned and non-learned motor-coordination behavior.

The differences between DAT-DTR (DT) and DAT:TH-KO mice in cue-dependent associative learning, spatial learning, spatial memory and object memory clearly indicate that other factors beyond striatal DA synthesis contribute to these behaviors. These factors could be (1) loss of physiological DA clearance due to reduction of striatal DAT expression after destruction of DA terminals, (2) loss of co-transmitters or modulators, like glutamate, serotonin, GABA or cholecystokinin, that have been reported to be released from DA terminals, (3) loss of trophic factors, e.g. brain-derived neurotrophic factor, that are produced by DA neurons, or (4) processes related to inflammation and/or gliosis that follow loss of DA neurons (Altar et al., 1997; Hnasko et al., 2010; Hokfelt et al., 1980; Nagatsu and Sawada, 2006; Seroogy et al., 1988; Seutin, 2005; Tritsch et al., 2012; Wallen-Mackenzie et al., 2010; Zhou et al., 2005).

Together with our previous findings (Darvas et al., 2014a; Darvas and Palmiter, 2011), and in agreement with other reports of striatal-DA related spatial- and associative-learning deficits (De Leonibus et al., 2007; Miyoshi et al., 2012; Miyoshi et al., 2002; Mura and Feldon, 2003), our current results suggest that (1) egocentric learning is quite resilient to effects of DA loss, (2) bradyphrenia, cognitive rigidity and spatial learning deficits require not only severe loss of striatal DA but also severe loss of nigro-striatal DA neurons, (3) severe loss of striatal DA alone is sufficient to cause cue-dependent associative learning defects, and (4) that cognitive deficits related to dysfunctional executive function, cognitive flexibility and working memory, already become apparent after mild-to-moderate loss of striatal DA and/or nigrostriatal DA neurons.

In conclusion, we suggest that as more striatal DA and nigro-striatal DA neurons are lost, cognitive performance in PD deteriorates and the resulting progressive impairment contributes to PDD. Further, the observed cognitive differences between severe loss of striatal DA vs. severe loss of nigro-striatal DA neurons establish the experimental basis for future studies aimed at determining which specific processes linked to the loss of DA neurons lead to the associated learning and memory impairments. Elucidating these processes will lead to a better understanding of the cognitive and motor deficits observed in late-stage PD and may inform the development of drugs that target novel non-DA factors, which could ultimately lead to more effective treatment regimens.

Acknowledgments

References

Aarsland D, Bronnick K, Larsen JP, Tysnes OB, Alves G. Cognitive impairment in incident, untreated Parkinson disease: the Norwegian ParkWest study. Neurology. 2009; 72:1121–1126. [PubMed: 19020293]

Altar CA, Cai N, Bliven T, Juhasz M, Conner JM, Acheson AL, Lindsay RM, Wiegand SJ. Anterograde transport of brain-derived neurotrophic factor and its role in the brain. Nature. 1997; 389:856–860. [PubMed: 9349818]

Antonini A, Tolosa E, Mizuno Y, Yamamoto M, Poewe WH. A reassessment of risks and benefits of dopamine agonists in Parkinson's disease. Lancet Neurol. 2009; 8:929–937. [PubMed: 19709931]

Bamford NS, Robinson S, Palmiter RD, Joyce JA, Moore C, Meshul CK. Dopamine modulates release from corticostriatal terminals. J. Neurosci. 2004; 24:9541–9552. [PubMed: 15509741]

Bevins RA, Besheer J. Object recognition in rats and mice: a one-trial non-matching-to-sample learning task to study 'recognition memory'. Nat. Protoc. 2006; 1:1306–1311. [PubMed: 17406415]

Borgkvist A, Malmlof T, Feltmann K, Lindskog M, Schilstrom B. Dopamine in the hippocampus is cleared by the norepinephrine transporter. Int. J. Neuropsychopharmacol. 2012; 15:531–540. [PubMed: 21669025]

Brozoski TJ, Brown RM, Rosvold HE, Goldman PS. Cognitive deficit caused by regional depletion of dopamine in prefrontal cortex of rhesus monkey. Science. 1979; 205:929–932. [PubMed: 112679]

Cheng F, Vivacqua G, Yu S. The role of alpha-synuclein in neurotransmission and synaptic plasticity. J. Chem. Neuroanat. 2011; 42:242–248. [PubMed: 21167933]

Cookson MR. alpha-Synuclein and neuronal cell death. Mol. Neurodegener. 2009; 4:9. [PubMed: 19193223]

D'Esposito M. From cognitive to neural models of working memory. Philos. Trans. R. Soc. Lond. B Biol. Sci. 2007; 362:761–772. [PubMed: 17400538]

Darvas M, Henschen CW, Palmiter RD. Contributions of signaling by dopamine neurons in dorsal striatum to cognitive behaviors corresponding to those observed in Parkinson's disease. Neurobiol. Dis. 2014a; 65:112–123. [PubMed: 24491966]

Darvas M, Palmiter RD. Restriction of dopamine signaling to the dorsolateral striatum is sufficient for many cognitive behaviors. Proc. Natl. Acad. Sci. U. S. A. 2009; 106:14664–14669. [PubMed: 19667174]

Darvas M, Palmiter RD. Restricting dopaminergic signaling to either dorsolateral or medial striatum facilitates cognition. J. Neurosci. 2010; 30:1158–1165. [PubMed: 20089924]

Darvas M, Palmiter RD. Contributions of striatal dopamine signaling to the modulation of cognitive flexibility. Biol. Psychiatry. 2011; 69:704–707. [PubMed: 21074144]

Darvas M, Wunsch AM, Gibbs JT, Palmiter RD. Dopamine dependency for acquisition and performance of Pavlovian conditioned response. Proc. Natl. Acad. Sci. U. S. A. 2014b; 111:2764–2769. [PubMed: 24550305]

De Leonibus E, Pascucci T, Lopez S, Oliverio A, Amalric M, Mele A. Spatial deficits in a mouse model of Parkinson disease. Psychopharmacology (Berl). 2007; 194:517–525. [PubMed: 17619858]

Fahn S. Description of Parkinson's disease as a clinical syndrome. Ann. N. Y. Acad. Sci. 2003; 991:1–14. [PubMed: 12846969]

Fearnley JM, Lees AJ. Ageing and Parkinson's disease: substantia nigra regional selectivity. Brain. 1991; 114(Pt 5):2283–2301. [PubMed: 1933245]

Henschen CW, Palmiter RD, Darvas M. Restoration of dopamine signaling to the dorsal striatum is sufficient for aspects of active maternal behavior in female mice. Endocrinology. 2013; 154:4316–4327. [PubMed: 23959937]

Hnasko TS, Chuhma N, Zhang H, Goh GY, Sulzer D, Palmiter RD, Rayport S, Edwards RH. Vesicular glutamate transport promotes dopamine storage and glutamate corelease in vivo. Neuron. 2010; 65:643–656. [PubMed: 20223200]

Hokfelt T, Rehfeld JF, Skirboll L, Ivemark B, Goldstein M, Markey K. Evidence for coexistence of dopamine and CCK in meso-limbic neurones. Nature. 1980; 285:476–478. [PubMed: 6105617]

Kalia LV, Brotchie JM, Fox SH. Novel nondopaminergic targets for motor features of Parkinson's disease: review of recent trials. Mov. Disord. 2013; 28:131–144. [PubMed: 23225267]

Kehagia AA, Barker RA, Robbins TW. Neuropsychological and clinical heterogeneity of cognitive impairment and dementia in patients with Parkinson's disease. Lancet Neurol. 2010; 9:1200–1213. [PubMed: 20880750]

Kim DS, Szczypka MS, Palmiter RD. Dopamine-deficient mice are hypersensitive to dopamine receptor agonists. J. Neurosci. 2000; 20:4405–4413. [PubMed: 10844009]

Koprich JB, Johnston TH, Reyes MG, Sun X, Brotchie JM. Expression of human A53T alpha-synuclein in the rat substantia nigra using a novel AAV1/2 vector produces a rapidly evolving pathology with protein aggregation, dystrophic neurite architecture and nigrostriatal degeneration with potential to model the pathology of Parkinson's disease. Mol. Neurodegener. 2010; 5:43. [PubMed: 21029459]

Lammel S, Hetzel A, Hackel O, Jones I, Liss B, Roeper J. Unique Properties of Mesoprefrontal Neurons within a Dual Mesocorticolimbic Dopamine System. Neuron. 2008; 57:760–773. [PubMed: 18341995]

Leverenz JB, Quinn JF, Zabetian C, Zhang J, Montine KS, Montine TJ. Cognitive impairment and dementia in patients with Parkinson disease. Curr. Top. Med. Chem. 2009; 9:903–912. [PubMed: 19754405]

Lima CF, Meireles LP, Fonseca R, Castro SL, Garrett C. The Frontal Assessment Battery (FAB) in Parkinson's disease and correlations with formal measures of executive functioning. J. Neurol. 2008; 255:1756–1761. [PubMed: 18821046]

Lundblad M, Decressac M, Mattsson B, Bjorklund A. Impaired neurotransmission caused by overexpression of alpha-synuclein in nigral dopamine neurons. Proc. Natl. Acad. Sci. U. S. A. 2012; 109:3213–3219. [PubMed: 22315428]

Maetzler W, Liepelt I, Berg D. Progression of Parkinson's disease in the clinical phase: potential markers. Lancet Neurol. 2009; 8:1158–1171. [PubMed: 19909914]

Miyoshi E, Wietzikoski EC, Bortolanza M, Boschen SL, Canteras NS, Izquierdo I, Da Cunha C. Both the dorsal hippocampus and the dorsolateral striatum are needed for rat navigation in the Morris water maze. Behav. Brain Res. 2012; 226:171–178. [PubMed: 21925543]

Miyoshi E, Wietzikoski S, Camplessei M, Silveira R, Takahashi RN, Da Cunha C. Impaired learning in a spatial working memory version and in a cued version of the water maze in rats with MPTP-induced mesencephalic dopaminergic lesions. Brain Res. Bull. 2002; 58:41–47. [PubMed: 12121811]

Morris R. Developments of a water-maze procedure for studying spatial learning in the rat. J. Neurosci. Methods. 1984; 11:47–60. [PubMed: 6471907]

Mura A, Feldon J. Spatial learning in rats is impaired after degeneration of the nigrostriatal dopaminergic system. Mov. Disord. 2003; 18:860–871. [PubMed: 12889075]

Nagatsu T, Sawada M. Cellular and molecular mechanisms of Parkinson's disease: neurotoxins, causative genes, and inflammatory cytokines. Cell. Mol. Neurobiol. 2006; 26:781–802. [PubMed: 16823625]

Nemani VM, Lu W, Berge V, Nakamura K, Onoa B, Lee MK, Chaudhry FA, Nicoll RA, Edwards RH. Increased expression of alpha-synuclein reduces neurotransmitter release by inhibiting synaptic vesicle reclustering after endocytosis. Neuron. 2010; 65:66–79. [PubMed: 20152114]

Owen AM, Beksinska M, James M, Leigh PN, Summers BA, Marsden CD, Quinn NP, Sahakian BJ, Robbins TW. Visuospatial memory deficits at different stages of Parkinson's disease. Neuropsychologia. 1993; 31:627–644. [PubMed: 8371837]

Postupna NO, Keene CD, Latimer C, Sherfield EE, Van Gelder RD, Ojemann JG, Montine TJ, Darvas M. Flow cytometry analysis of synaptosomes from post-mortem human brain reveals changes specific to Lewy body and Alzheimer's disease. Lab. Invest. 2014; 94:1161–1172. [PubMed: 25068655]

Ragozzino ME. The effects of dopamine D(1) receptor blockade in the prelimbic-infralimbic areas on behavioral flexibility. Learn. Mem. 2002; 9:18–28. [PubMed: 11917003]

Retailleau A, Dejean C, Fourneaux B, Leinekugel X, Boraud T. Why am I lost without dopamine? Effects of 6-OHDA lesion on the encoding of reward and decision process in CA3. Neurobiol. Dis. 2013; 59:151–164. [PubMed: 23911573]

Samii A, Nutt JG, Ransom BR. Parkinson's disease. Lancet. 2004; 363:1783–1793. [PubMed: 15172778]

Schapira AHV, Olanow CW, Greenamyre JT, Bezard E. Slowing of neurodegeneration in Parkinson's disease and Huntington's disease: future therapeutic perspectives. Lancet. 2014; 384:545–555. [PubMed: 24954676]

Scherman D, Desnos C, Darchen F, Pollak P, Javoy-Agid F, Agid Y. Striatal dopamine deficiency in Parkinson's disease: role of aging. Ann. Neurol. 1989; 26:551–557. [PubMed: 2817829]

Seroogy K, Ceccatelli S, Schalling M, Hokfelt T, Frey P, Walsh J, Dockray G, Brown J, Buchan A, Goldstein M. A subpopulation of dopaminergic neurons in rat ventral mesencephalon contains both neurotensin and cholecystokinin. Brain Res. 1988; 455:88–98. [PubMed: 3046712]

Seutin V. Dopaminergic neurones: much more than dopamine? Br. J. Pharmacol. 2005; 146:167–169. [PubMed: 16025140]

Tritsch NX, Ding JB, Sabatini BL. Dopaminergic neurons inhibit striatal output through non-canonical release of GABA. Nature. 2012; 490:262–266. [PubMed: 23034651]

Voon V, Mehta AR, Hallett M. Impulse control disorders in Parkinson's disease: recent advances. Curr. Opin. Neurol. 2011; 24:324–330. [PubMed: 21725242]

Vorhees CV, Williams MT. Morris water maze: procedures for assessing spatial and related forms of learning and memory. Nat. Protoc. 2006; 1:848–858. [PubMed: 17406317]

Wallen-Mackenzie A, Wootz H, Englund H. Genetic inactivation of the vesicular glutamate transporter 2 (VGLUT2) in the mouse: what have we learnt about functional glutamatergic neurotransmission? Ups. J. Med. Sci. 2010; 115:11–20. [PubMed: 20187846]

Whitton PS. Inflammation as a causative factor in the aetiology of Parkinson's disease. Br. J. Pharmacol. 2007; 150:963–976. [PubMed: 17339843]

Williams-Gray CH, Foltynie T, Brayne CE, Robbins TW, Barker RA. Evolution of cognitive dysfunction in an incident Parkinson's disease cohort. Brain. 2007; 130:1787–1798. [PubMed: 17535834]

Zhou FM, Liang Y, Salas R, Zhang L, De Biasi M, Dani JA. Corelease of dopamine and serotonin from striatal dopamine terminals. Neuron. 2005; 46:65–74. [PubMed: 15820694]

Highlights

- Severe loss of striatal dopamine causes cognitive impairment resembling advanced PD

- Loss of dopamine neurons causes more cognitive deficits than loss of dopamine alone

- Severe loss of striatal dopamine is sufficient to cause extensive motor defects
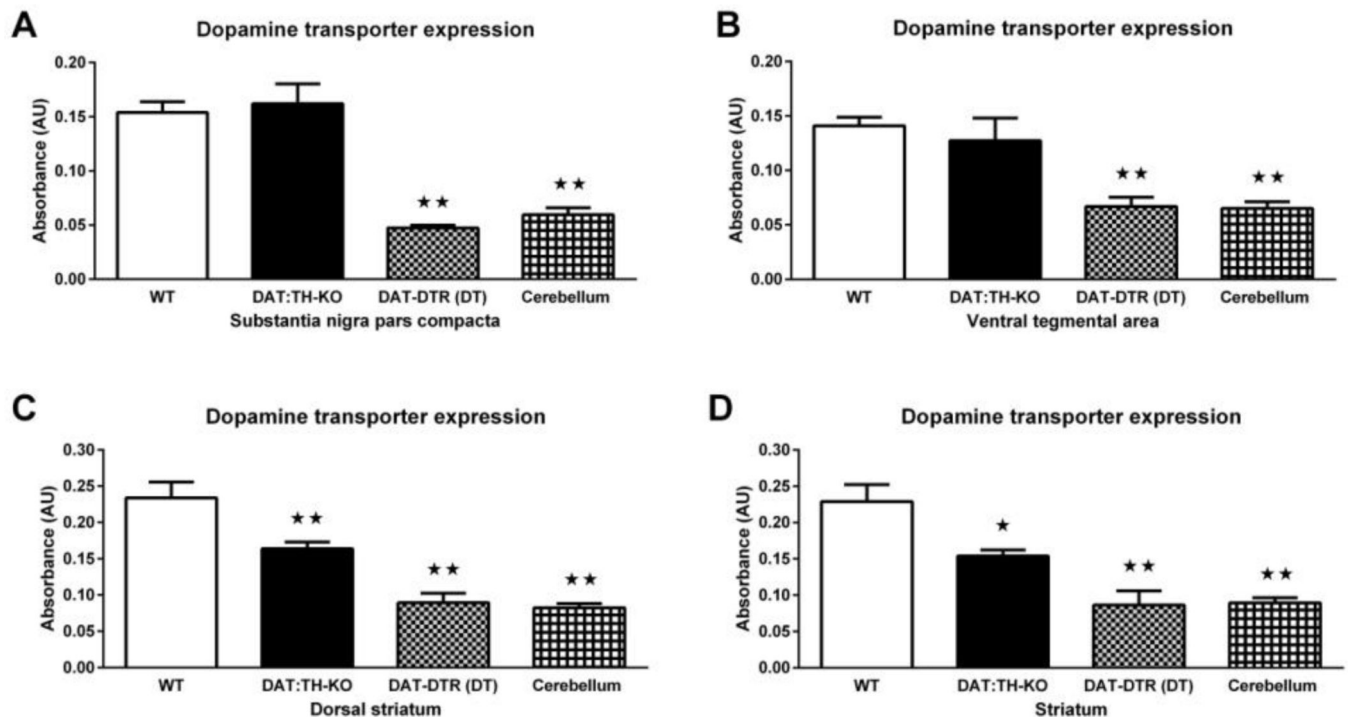
Fig. 1.
DAT expression in midbrain and striatum measured by ELISA. (A) DAT expression in SNpc dissections from WT (N = 11), DAT:TH-KO (N = 4) and DAT-DTR (DT) (N = 6) mice. (B) DAT expression in VTA dissections from WT (N = 11, DAT:TH-KO (N = 4) and DAT-DTR (DT) (N = 4) mice. (C) DAT expression in tissue punches containing dorsal striatum from WT (N = 6), DAT:TH-KO (N = 6) and DAT-DTR (DT) (N = 6) mice. (C) DAT expression in tissue punches containing ventral striatum from WT (N = 6), DAT:TH-KO (N = 6) and DAT-DTR (DT) (N = 6) mice. As a negative control, DAT-expression in WT cerebellum is also shown. Midbrain samples were analyzed together with one set of cerebellar WT samples (n = 6), and striatal samples were analyzed together with an additional set of cerebellar WT samples (n = 6). Significant differences from control groups are marked with stars (★★ $p < 0.01$). All data are shown as means ± SEM.
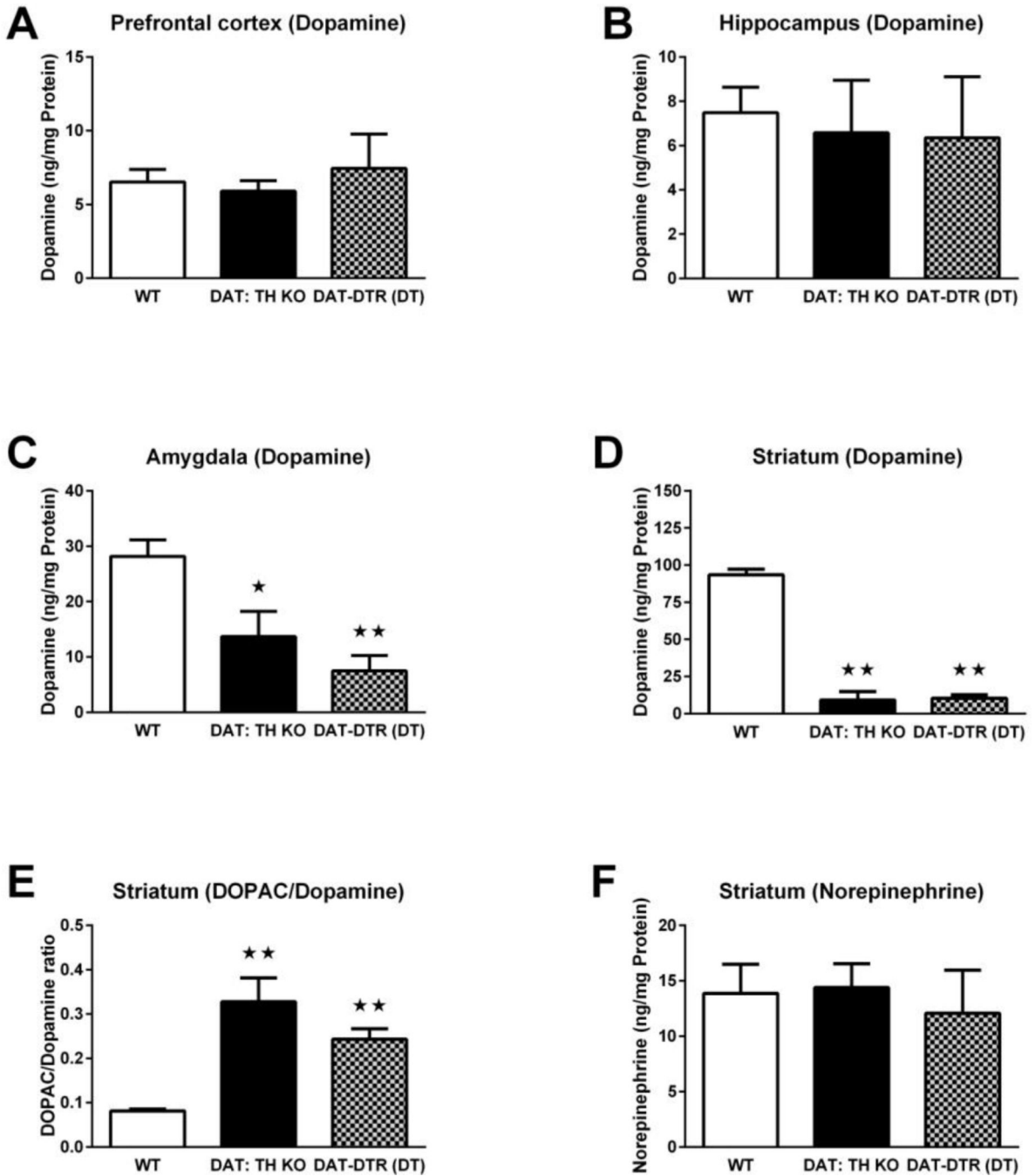
Fig. 2.
Tissue content of DA, the DOPAC/DA ratio and tissue content of norepinephrine in DA projection fields. (A) DA content in the prefrontal cortex of WT (N = 24), DAT:TH-KO (N = 4) and DAT-DTR (DT) (N = 8) mice. (B) DA content in the hippocampus of WT (N = 10), DAT:TH-KO (N = 4) and DAT-DTR (DT) (N = 2) mice. (C) DA content in the amygdala of WT (N = 21), DAT:TH-KO (N = 14) and DAT-DTR (DT) (N = 7) mice. (D) DA content in the striatum of WT (N = 22), DAT:TH-KO (N = 10) and DAT-DTR (DT) (N = 17) mice. (E) DOPAC/DA ratio in the striatum of WT (N = 21), DAT:TH-KO (N = 10)

and DAT-DTR (DT) (N = 12) mice. (F) Norepinephrine levels in the striatum of WT (N = 20), DAT:TH-KO (N = 13) and DAT-DTR (DT) (N = 5) mice. Significant differences from control groups are marked with stars (★★ p < 0.01, ★ p < 0.05). All data are shown as means ± SEM.
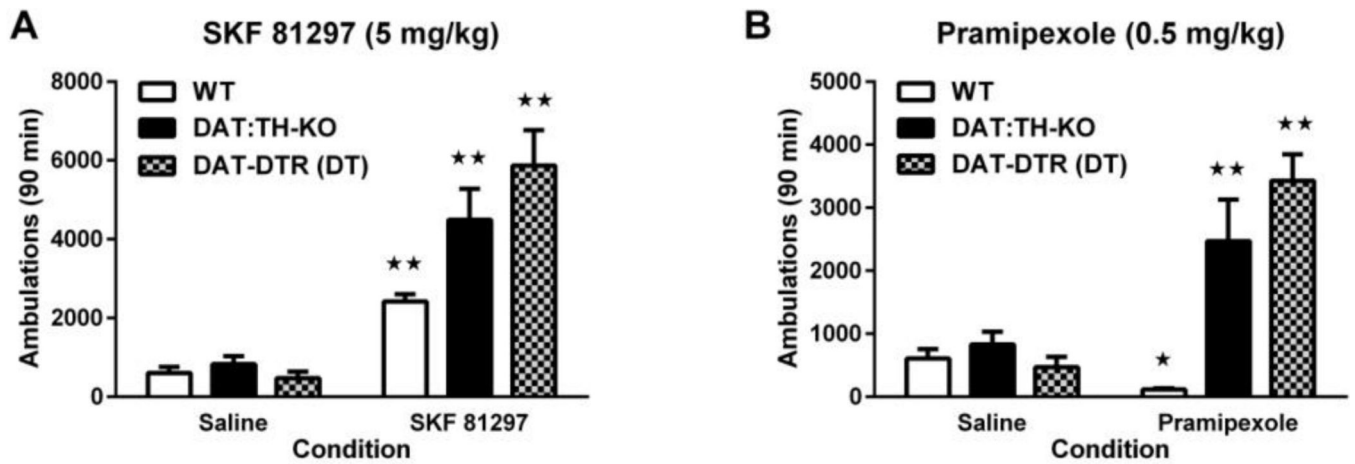
Fig. 3.

Locomotor response to DA-receptor agonists. (A) Locomotor ambulations in response to the D1 DA-receptor agonist SKF 81297 and to saline by WT (N = 14–21), DAT:TH-KO (N = 9–12) and DAT-DTR (DT) (N = 6–7) mice. (B) Locomotor ambulation in response to the D2/D3 DA-receptor agonist pramipexole and to saline by WT (N = 18–21), DAT:TH-KO (N = 8–12) and DAT-DTR (DT) (N = 5–6) mice. Significant differences in drug-elicited ambulation compared with ambulation after saline administration are marked with stars (★★ $p < 0.01$, ★ $p < 0.05$). All data are shown as means ± SEM.
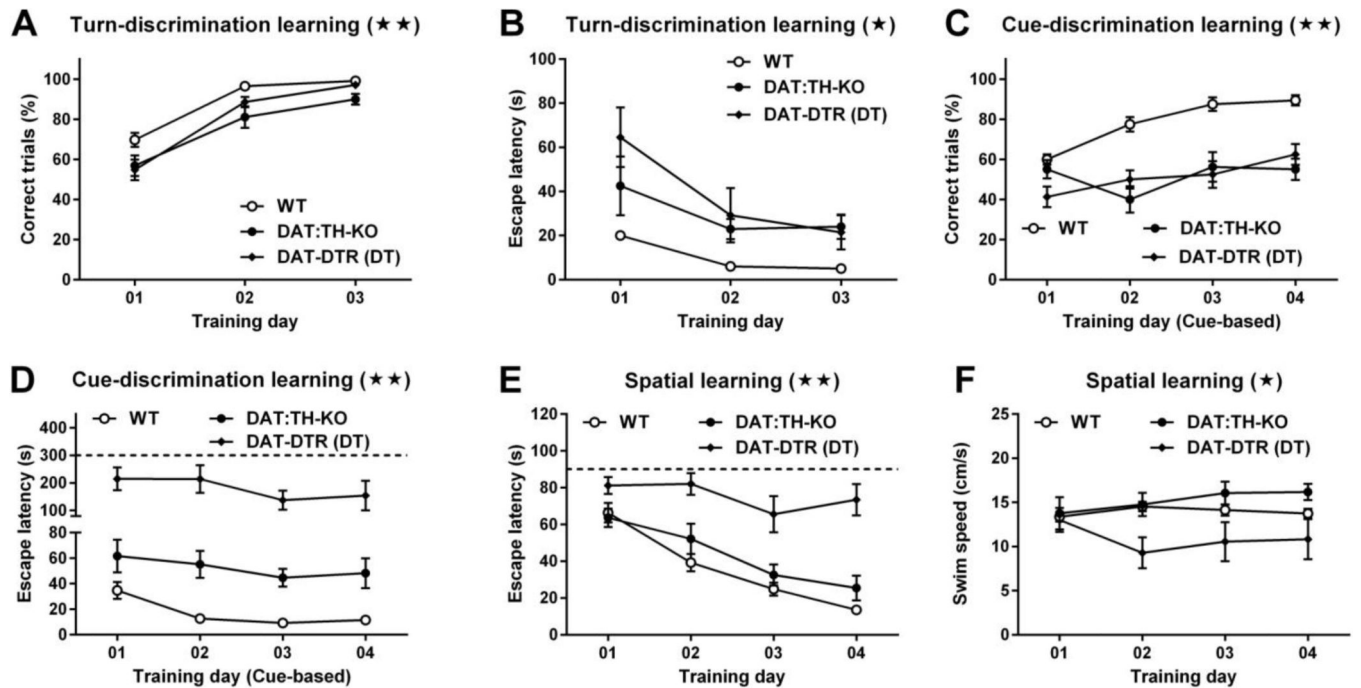
Fig. 4.

Turn- dependent, cue-dependent and spatial learning. Panels A–B show turn-dependent learning data from WT (N = 34), DAT:TH-KO (N = 19) and DAT-DTR (DT) (N = 21) mice. (A) Percentage of correct trials and (B) latency to climb onto the platform during 3-day training of turn-based water escape in the U-shaped water maze. Panels C–D show cue-dependent learning data from WT (N = 16), DAT:TH-KO (N = 8) and DAT-DTR (DT) (N = 8) mice. (C) Percentage of correct trials and (D) latency to climb onto the platform during 4-day training of cue-based water escape in the U-shaped water maze. (E) Latency to climb onto the hidden platform during training of spatial learning in the Morris water maze by WT (N = 18), DAT:TH-KO (N = 8) and DAT-DTR (DT) (N = 9) mice. (F) Swim speed of WT (N = 18), DAT:TH-KO (N = 8) and DAT-DTR (DT) (N = 9) mice in the Morris water maze procedure. Significant group effects for all learning tests are marked with stars in the panel titles (★★ $p < 0.01$, ★ $p < 0.05$). All data are shown as means ± SEM.
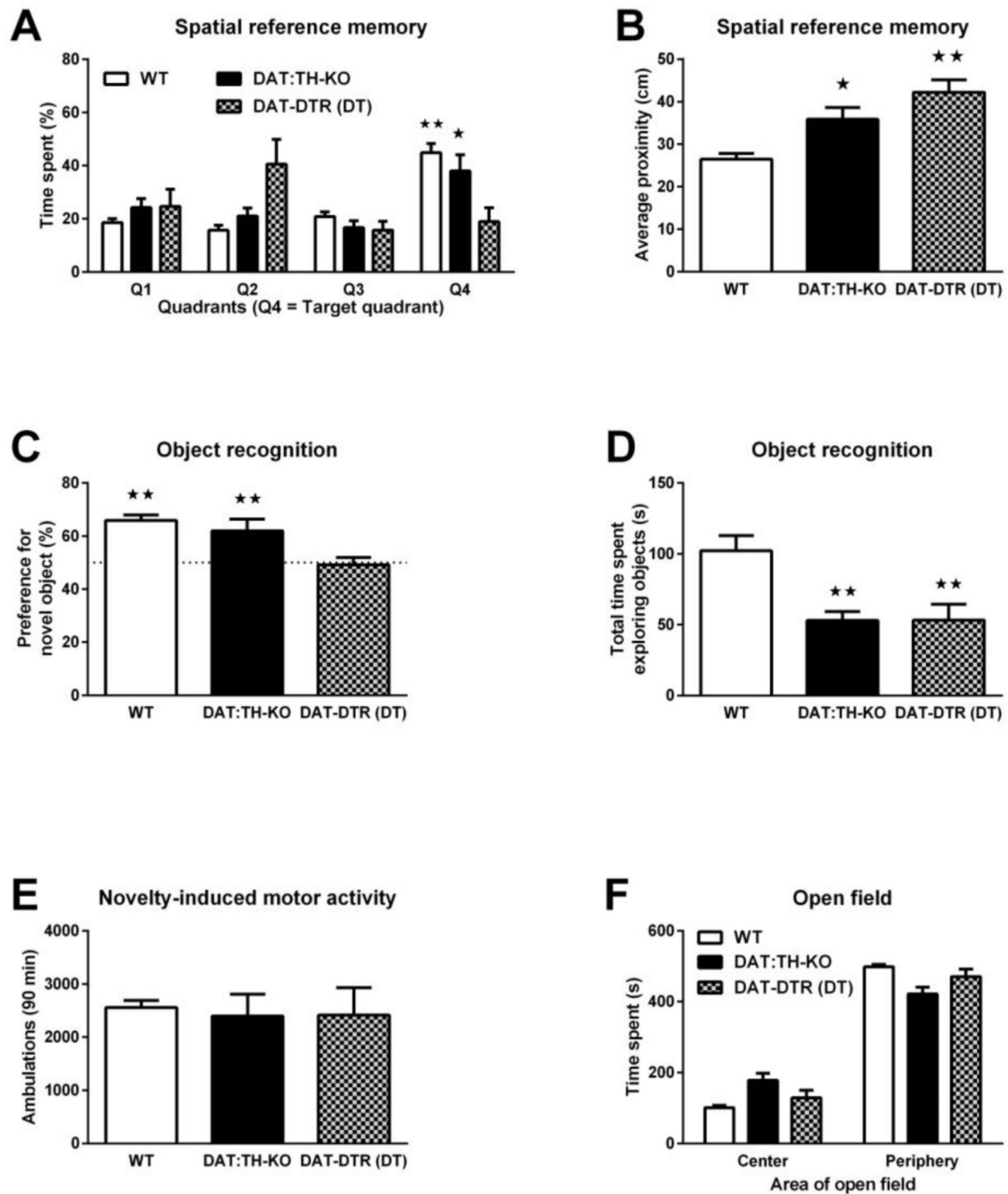
Fig. 5.
Spatial reference memory, object memory and anxiety. (A) Time spent in the quadrants of the Morris water maze 24 h after the last of 4 training days. Data are shown for WT (N = 18), DAT:TH-KO (N = 8) and DAT-DTR (DT) (N = 9) mice. Q4 denotes the quadrant in which the platform was located during previous training sessions. (B) Average proximity to the exact platform position 24 h after the last of 4 training days. Data are shown for WT (N = 18), DAT:THKO (N = 8) and DAT-DTR (DT) (N = 9) mice. (C) Percentage of total exploration time spent with the novel object in WT (N = 14), DAT:TH-KO (N = 11) and

DAT-DTR (DT) (N = 5) mice during a choice preference test 24 h after mice were habituated to the non-novel object. (D) Total time spent exploring both objects during the choice preference test by WT (N = 14), DAT:TH-KO (N = 11) and DAT-DTR (DT) (N = 9 mice. (E) Locomotor ambulations in response to novelty by WT (N = 26), DAT:TH-KO (N = 24) and DAT-DTR (DT) (N = 6) mice. (F) Anxiety, scored as time spent in the center zone and periphery of an open-field arena, by WT (N = 23), DAT:TH-KO (N = 15) and DAT-DTR (DT) (N = 12) mice. For spatial reference memory in (A), significant differences in time spent in quadrant Q4 compared with all other quadrants are marked with stars (★★ $p < 0.01$, ★ $p < 0.05$). The dashed line in (C) marks a hypothetical 50% preference (i.e. indifference) for the novel object and percentages that differ significantly from that value are marked with stars (★★ $p < 0.01$). For all other panels, significant differences from control groups are marked with stars (★★ $p < 0.01$, ★ $p < 0.05$). All data are shown as means ± SEM.
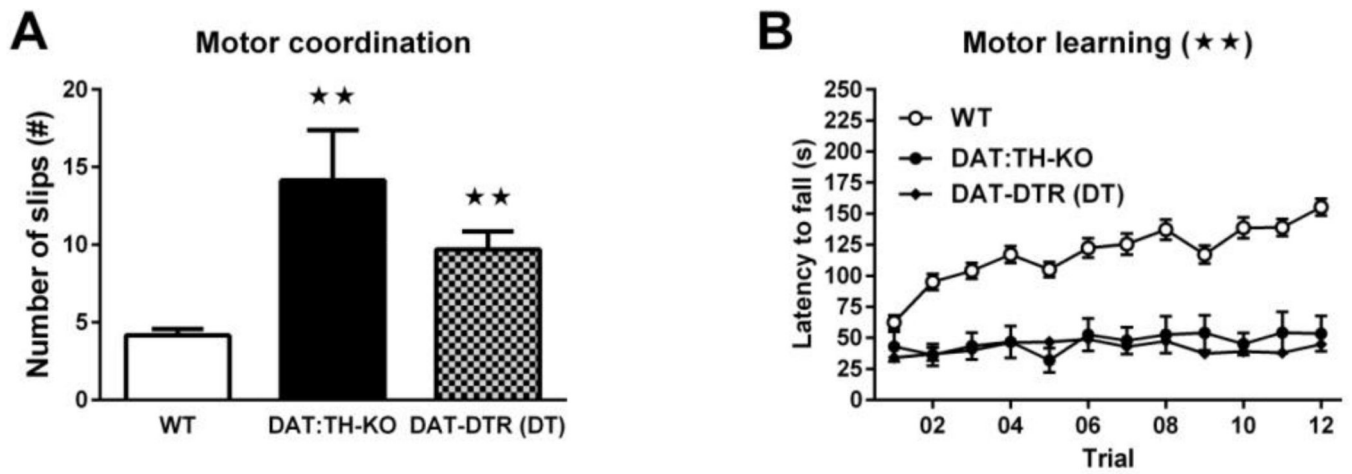
Fig. 6.

Motor coordination and motor learning. (A) Number of slips during the balance-beam test of learning-independent motor coordination by WT (N = 25), DAT:TH-KO (N = 7) and DAT-DTR (DT) (N = 13) mice. (B) Latency to fall from an accelerating rotarod during motor-skill learning by WT (N = 32), DAT:TH-KO (N = 7) and DAT-DTR (DT) (N = 29) mice. For the beam walk test (A), significant differences from WT mice are marked with stars (★★ p < 0.01). Significant group effects for the rotarod test (B) are marked with a star in the panel title (★★ p < 0.01). All data are shown as means ± SEM. All data are shown as means ± SEM.